HHS Public Access

Author manuscript

J Biomed Mater Res A. Author manuscript; available in PMC 2018 March 01.

Published in final edited form as:

J Biomed Mater Res A. 2017 March ; 105(3): 770–778. doi:10.1002/jbm.a.35947.

Effect of Matrix Metalloproteinase-Mediated Matrix Degradation on Glioblastoma Cell Behavior in 3D PEG-based Hydrogels

Christine Wang[a], **Xinming Tong, Ph.D.**[b], **Xinyi Jiang, Ph.D.**[b], and **Fan Yang, Ph.D.**[a,b,*]

[a]Department of Bioengineering, Stanford University, Stanford, CA 94305, USA

[b]Department of Orthopaedic Surgery, Stanford University, Stanford, CA 94305, USA

Abstract

Glioblastoma (GBM) is the most common and aggressive form of primary brain tumor with median survival of 12 months. To improve clinical outcomes, it is critical to develop *in vitro* models that support GBM proliferation and invasion for deciphering tumor progression and screening drug candidates. A key hallmark of GBM cells is their extreme invasiveness, a process mediated by matrix metalloproteinase (MMP)-mediated degradation of the extracellular matrix. We recently reported the development of a MMP-degradable, poly(ethylene-glycol)-based hydrogel platform for culturing GBM cells. In the present study, we modulated the percentage of MMP-degradable crosslinks in 3D hydrogels to analyze the effects of MMP-degradability on GBM fates. Using an immortalized GBM cell line (U87) as a model cell type, our results showed that MMP-degradability was not required for supporting GBM proliferation. All hydrogel formulations supported robust GBM proliferation, up to 10 fold after 14 days. However, MMP-degradability was essential for facilitating tumor spreading, and 50% MMP-degradable hydrogels were sufficient to enable both robust tumor cell proliferation and spreading in 3D. The findings of this study highlight the importance of modulating MMP-degradability in engineering 3D *in vitro* brain cancer models and may be applied for engineering *in vitro* models for other cancer types.

Keywords

Matrix metalloproteinase; glioblastoma; degradable hydrogels; cancer model; three-dimensional

INTRODUCTION

Glioblastoma (GBM) is the most common and aggressive form of primary brain tumor in adults. Despite aggressive treatment regimens, patients continue to face a median survival of 12 months and a 5-year survival rate of 4%.[1–3] A key hallmark of GBM cells is their extreme ability to invade and migrate into neighboring tissue, precluding complete surgical

*Corresponding author: Fan Yang, Ph.D., Assistant Professor of Orthopaedic Surgery and Bioengineering, Stanford University, 300 Pasteur Dr., Edwards R105, Stanford, CA, 94305-5341, Tel: 650-725-7128, Fax: 650-723-9370, fanyang@stanford.edu.
Christine Wang, Stanford University, 300 Pasteur Dr., Edwards R114, Stanford, CA, 94305-5341, Tel: 650-498-6847, Fax: 650-723-9370, wachris@stanford.edu
Xinming Tong, Ph.D., Stanford University, 300 Pasteur Dr., Edwards R114, Stanford, CA, 94305-5341, Tel: 650-498-6847, Fax: 650-723-9370, xinming@stanford.edu
Xinyi Jiang, Ph.D., Stanford University, 300 Pasteur Dr., Edwards R114, Stanford, CA, 94305-5341, Tel: 650-498-6847, Fax: 650-723-9370, jiangxy@stanford.edu

removal of the tumor and leading to eventual tumor recurrence. 96% of patients will experience tumor recurrence at or within 2 cm of the margin of surgical tumor resection.[4] To better understand brain tumor progression and improve clinical outcomes for patients, there is a critical need for *in vitro* culture models for deciphering tumor biology, as well as drug screening. Currently, the gold standard models are 2D monolayer culture and organotypic culture. Although 2D monolayer culture is low cost and convenient, such a model does not fully recapitulate the *in vivo* 3D extracellular matrix (ECM) architecture and does not permit studies of cell invasion in 3D. Alternatively, organotypic culture contains many ECM cues found *in vivo*, but offers little tunability of the inputs and can be low-throughput due to tissue availability and processing times.

Using the principles of tissue engineering, previous literature and our prior work have demonstrated the potential for biomaterials-based hydrogels as 3D *in vitro* tumor models.[5–11] Such models can mimic native ECM architecture and composition, thereby providing a culture platform for studying tumor cell behavior in a physiologically-relevant and controllable manner. Hydrogels have high tissue-mimicking water content and are highly tunable, permitting mechanistic studies of various niche cues on tumor cell behavior in 3D. Previous literature has investigated the effects of varying mechanical or biochemical cues on GBM tumor cell behavior. For example, hyaluronic acid (HA) is the main component of brain ECM, and, in HA-based hydrogels, GBM tumor cells displayed stiffness-dependent cell migration patterns.[5] In addition, in collagen I-based hydrogels, increasing collagen content led to decreased GBM tumor cell proliferation due to increased hydrogel crosslinking density.[10] Lastly, in gelatin-based hydrogels, increasing hydrogel stiffness led to increased GBM tumor cell proliferation and spreading.[9] These pioneering studies have elucidated significant insight into the effects of various tumor niche cues on GBM cell fates. While the degradability of the matrix plays an important role in GBM cell migration and invasion, previous studies did not vary hydrogel degradability in a controlled manner. As such, how matrix degradability would influence GBM cell invasion remains largely unknown.

GBM tumor cells are known to actively invade and infiltrate as single cells into neighboring tissue along the basal lamina of blood vessels or white matter tracts.[12] To invade through the dense brain extracellular matrix (ECM), GBM tumor cells utilize matrix metalloproteinases (MMP), which can degrade various ECM proteins, including fibronectin, laminin, collagen, or gelatin.[13] GBM cells are known to secrete various MMPs, including MMP1, MMP2, or MMP9,[14–16] and upregulation of MMP expression has been shown to correlate with brain tumor grade and lower survival.[17] Inhibition of various MMPs has been demonstrated to significantly decrease tumor cell invasion *in vitro* and tumor formation *in vivo.*[12] These observations support the notion that MMPs play important roles in GBM tumor progression and the dissemination of tumor cells throughout brain tissue.

Given the pivotal roles of MMPs in GBM tumors, 3D hydrogel-based culture models should support MMP-mediated degradation by tumor cells. Previous literature has demonstrated the potential for introducing MMP degradability in engineered polyethylene glycol (PEG)-based hydrogels using MMP-degradable peptide crosslinkers.[18] Furthermore, the authors demonstrated that fibroblasts showed increased cell spreading and proliferation when the

MMP-degradability of 3D hydrogels was increased.[18] Recently, we reported a MMP-degradable, PEG-based hydrogel system for culturing GBM cells in 3D.[11] How the degree of MMP-degradability influences GBM tumor cell behavior remains largely unknown. The goal of this study was to analyze the effects of varying the percentage of MMP-degradable crosslinks (0%, 50%, and 100%) in 3D PEG-based hydrogels to determine an optimal hydrogel formulation that can support robust tumor cell proliferation and spreading. 8-arm PEG-norbornene (PEG-NB) molecules were used for hydrogel fabrication, which can be crosslinked with a MMP-degradable peptide crosslinker (CGPQGIWGQC) and a non-degradable PEG-dithiol crosslinker (PEG-SH). The ratio between the two crosslinkers was tuned to achieve varying percentages of MMP-degradability (0%, 50%, or 100% MMP-degradable). To allow for cell adhesion to the hydrogel network, a cell adhesion peptide (CRGDS) was chemically conjugated to PEG-NB molecules. HA is the main component of brain ECM,[17] and to mimic the brain ECM, thiol-modified sodium hyaluronate (HA-SH) (20 – 40 kDa) was chemically incorporated into the hydrogel network. Thiol-ene UV photopolymerization was used to induce hydrogel gelation, as this process has been shown to be cytocompatible and permits spatial and temporal control.[19] Hydrogels with varying percentages of MMP-degradability were characterized using a degradation assay in collagenase solution, mechanical testing, and quantification of equilibrium swell ratio. For cell studies, an immortalized GBM cell line (U87) was used as a model cell type and cultured in PEG hydrogels with varying percentages of MMP-degradable crosslinks for 14 days. Cell proliferation was monitored using brightfield microscopy and was quantified via cell DNA content in the hydrogels after 14 days. Cell morphology was analyzed using brightfield and confocal microscopy. Gene expression levels of ECM-remodeling proteins, specifically MMPs and HA synthases, were quantified using RT-PCR.

MATERIALS AND METHODS

Materials

8-arm PEG (MW ~ 40 kDa) was purchased from JenKem Technology USA (Allen, TX, USA). Linear PEG (MW ~ 1.5 kDa) was purchased from Sigma-Aldrich USA (St. Louis, MO, USA). RGD peptide (CRGDS) was purchased from Bio Basic, Inc (Amherst, NY, USA). Sodium hyaluronate (HA) (MW ~ 20–40 kDa) was purchased from Lifecore Biomedical (Chaska, MN, USA). MMP-degradable peptide (CGPQGIWGQC) was purchased from GenScript (Piscataway, NJ, USA). 8-arm PEG-norbornene (PEG-NB) and linear PEG-dithiol (PEG-SH) were synthesized as previously reported.[19,20] Thiolated sodium hyaluronate (HA-SH) was synthesized as previously reported.[21] All other reagents were obtained from Fisher Scientific (Pittsburgh, PA, USA) unless otherwise noted.

Hydrogel fabrication

8-arm PEG-NB (40 kDa) was used, which can be crosslinked with non-degradable linear PEG-SH (1.5 kDa) and MMP-degradable peptide (CGPQGIWGQC). 2 of 8 arms on PEG-NB were used for conjugation of biochemical cues. The remaining 6 arms on PEG-NB were used for crosslinking with non-degradable linear PEG-SH and MMP-degradable peptide. To tune the percentage of MMP-degradable crosslinks (0%, 50%, and 100% MMP-degradable), 8-arm PEG-NB, linear PEG-SH, and MMP-degradable peptide were mixed at varying molar

ratios (Table S1). For cell adhesion, RGD peptide (CRGDS) was covalently linked to the hydrogel network at a final concentration of 0.914 mM. To mimic brain ECM content, thiol-modified sodium hyaluronate (HA-SH) was added at a final concentration of 0.004% (w/v), which was selected based on reported values of hyaluronic acid content in human brain tissue.[22] To induce hydrogel formation via thiol-ene photopolymerization, hydrogel components were mixed together in the presence of photoinitiator Igracure D2959 (0.05% w/v, Ciba Specialty Chemicals, Tarrytown, NY, USA). Each hydrogel sample contained 75 μL of hydrogel precursor solution, which was loaded in a cylindrical-shaped mold (3 mm in height, 5 mm in diameter). To induce gelation, hydrogels were exposed to UV light (365 nm, 4mW/cm^2) for 5 min at room temperature.

Measurement of diffusion of unbound HA-SH

HA-SH was fluorescently labeled with fluorescein-maleimide (Sigma) overnight at room temperature, such that 3.33% of the -SH groups were labeled. To measure the diffusion of unbound HA-SH over time, hydrogels were fabricated as above and placed in PBS at 37°C (n = 3). Supernatant was removed at the following timepoints: 0.5, 2, 24, 120, and 168 hrs. At each timepoint, the fluorescence signal of the supernatant was measured using a plate reader (excitation λ = 494 nm, emission λ = 521 nm) (Molecular Devices, Sunnyvale, CA, USA).

Hydrogel characterization

To analyze the degradation profiles of the hydrogels with varying percentages of MMP-degradability, acellular hydrogels were prepared as above and equilibrated in PBS at 37°C overnight (n = 3). Hydrogels were transferred to either a solution of collagenase (Type II, 1 U/ml, Worthington Biochemical Corp, Lakewood, NJ, USA) or PBS only control. The wet weight of the hydrogel was measured at 0, 1, 2, 3, 4, 6, and 7 hrs. The starting timepoint was defined as the time after hydrogels have reached equilibrium following overnight incubation.

To measure the stiffness of hydrogels with varying percentages of MMP-degradability, acellular hydrogels prepared as above were allowed to equilibrate overnight at room temperature for measuring the hydrogel stiffness on Day 1 (n = 3). Unconfined compressive tests were conducted using an Instron 5944 materials testing system (Instron Corporation, Norwood, MA, USA). The test set-up consisted of custom made aluminum compression plates lined with PTFE to minimize friction. All tests were conducted in PBS solution at RT. Hydrogel diameter and thickness were measured using digital calipers and the material testing system's position read-out, respectively. Before each test, a preload of approximately 2 mN was applied. The upper plate was then lowered at a rate of 1% strain/sec to a maximum strain of 30%. Load and displacement data were recorded at 100 Hz. The modulus was determined for strain ranges of 10–20% from linear curve fits of the stress vs. strain curve in each strain range.

To calculate equilibrium swelling ratio Q and theoretical mesh size of hydrogels with varying MMP-degradability, acellular hydrogels prepared as above were allowed to equilibrate in PBS at room temperature overnight (n = 3). The wet weight of the hydrogel was measured after overnight incubation, by which the hydrogels have reached equilibrium.

Hydrogels were subsequently lyophilized for 48 hrs, and dry weight was measured. The equilibrium swelling ratio Q was calculated as the ratio of the mass of the swollen hydrogel to the mass of the dry components after lyophilization. The theoretical hydrogel mesh size was calculated as done previously, based on the Flory-Rehner calculation.[23]

Cell encapsulation

U87-MG cells (U87) were expanded in standard growth medium consisting of Dulbecco's minimal essential medium (DMEM, Life Technologies, Carlsbad, CA, USA), supplemented with 10% (v/v) fetal bovine serum (FBS, Gibco, Life Technologies), 100 units/ml penicillin (Life Technologies), and 100 μg/ml streptomycin (Life Technologies) at 37°C in 5% CO_2. For encapsulation in hydrogels, trypsinized cells were resuspended in the hydrogel precursor solution at a final concentration of 0.5M cells/ml. 75 μL of the cell-containing hydrogel solution was pipetted into a cylindrical-shaped mold and UV crosslinked as described above. The samples were then cultured in growth medium as described above for 14 days at 37°C in 5% CO_2 with media change every other day.

Cell proliferation

Cell proliferation was monitored over 14 days using bright field microscopy (Zeiss, Jena, Germany). To quantify fold change in cell proliferation, cell DNA content in hydrogels at Days 1 and 14 was measured using the Quant-iT PicoGreen assay (Life Technologies). Briefly, lyophilized hydrogel samples were rehydrated and digested using papain (Worthington Biochemical Corp) at 60°C for 16 hrs (n = 3). After cooling to room temperature, samples were vortexed and centrifuged at 10,000 rpm for 5 min. The supernatant was used to measure total DNA content per hydrogel using PicoGreen assay (Life Technologies) per manufacturer's instructions.

Gene expression

Gene expression levels of MMPs (MMP1, MMP2, and MMP9) and HA synthases (HAS1, HAS2, and HAS3) were analyzed on Days 1 and 14. To measure the expression of target genes, total RNA was extracted from the hydrogels, and RT-PCR was performed using primers as described previously (n = 3).[11] Briefly, hydrogel samples were homogenized in TRIzol (Life Technologies). RNA was extracted by the addition of chloroform and precipitated using RNeasy Mini Kit columns (Qiagen, Valencia, CA, USA). cDNA was synthesized from extracted RNA using SuperScript III First-Strand Synthesis kit (Life Technologies) per manufacturer's instructions. RT-PCR was then performed on an Applied Biosystems 7900 Real-Time PCR system (Applied Biosystems, Life Technologies) using Power SYBR Green PCR Master Mix (Applied Biosystems, Life Technologies) per manufacturer's instructions. Relative expression levels of target genes were determined using the comparative C_T method. Target gene expression was first normalized to an endogenous gene GAPDH, followed by a second normalization to the gene expression level on Day 1.

Immunostaining

For F-actin immunostaining, cell-laden hydrogels were fixed in 4% paraformaldehyde (Sigma) for 1 hr at 37°C (n = 2). Cells were then permeabilized in PBS containing 0.1% Triton X-100 (Sigma) for 1 hr at 37°C. Nonspecific binding was blocked using 1% BSA/ 0.1% Triton X-100 in PBS overnight at 37°C. To stain for F-actin, cells were stained with phalloidin-rhodamine (50 μg/ml, Sigma) for 1 hr at 37°C. Cell nuclei were counterstained with Hoechst dye 33342 (0.25 μg/ml, Cell Signaling Technologies, Danvers, MA, USA) for 1 hr at 37°C. Gels were then incubated in mounting media overnight at 4°C (Vectashield, Vector Laboratories, Burlingame, CA, USA) and imaged using confocal microscope (Leica SP5, Leica, Wetzlar, Germany).

Statistical analyses

GraphPad Prism (GraphPad software, San Diego, CA, USA) was used to perform statistical analysis on cell proliferation and theoretical mesh size data. Unpaired student's t-tests (assuming Gaussian distribution) and two-way analysis of variance (ANOVA) with Tukey's multiple comparisons test were used to determine statistical significance ($p < 0.05$). Error was reported as standard deviation unless otherwise noted.

RESULTS

Characterization of materials and hydrogel properties

To achieve stable incorporation of hyaluronic acid (HA) within the hydrogel network, crosslinkable thiol groups were introduced onto sodium hyaluronate, as previously reported.[21] NMR spectroscopy confirmed successful incorporation of thiol groups on sodium hyaluronate (Figure S1A). Minimal amount of HA-SH diffused after 7 days (0.4% diffused), confirming stable HA-SH incorporation in 3D hydrogels (Figure S1B).

Hydrogels with varying percentages of MMP-degradability had stiffnesses ranging from 1.2 to 2.0 kPa, which is within the range reported for normal brain tissue (Figure 1C).[24,25] The equilibrium swelling ratio (Q) was measured to calculate the theoretical mesh size for hydrogels of varying MMP-degradability using the Flory-Rehner calculation.[23] Hydrogels with varying percentages of MMP-degradability had comparable equilibrium swelling ratios Q (30.43 – 32.68) and theoretical mesh sizes (14.72 – 15.18 nm) (Figure 1D, E).

To characterize MMP-mediated degradation profiles, hydrogels with varying percentages of MMP-degradability were incubated in collagenase solution (Figure 1B). 0% MMP-degradable hydrogels did not have any change in wet weight, indicating the lack of MMP-dependent degradation. The wet weight of 50% MMP-degradable hydrogels increased over time, indicating hydrogel swelling due to degradation. Lastly, 100% MMP-degradable hydrogels decreased in wet weight, indicating loss of hydrogel mass due to degradation.

Effects of MMP-degradability on GBM cell proliferation

Using an immortalized GBM cell line U87 as a model cell type, the effects of varying percentages of MMP-degradability on tumor cell proliferation were analyzed over 14 days (Figure 2). In all hydrogel formulations, U87 cells started as single cells after encapsulation

on Day 1 and formed large multicellular aggregates by Day 14 (Figure 2A). All hydrogel formulations supported robust tumor cell proliferation, up to 10-fold increases in DNA content after 14 days (Figure 2B).

Effects of MMP-degradability on GBM cell morphology

A key hallmark of GBM cells is their extreme ability to invade into neighboring tissue. Degradation of the surrounding ECM is an important player in permitting GBM cell protrusions and spreading, a prerequisite for cell migration. The effects of varying percentages of MMP-degradability on tumor cell morphology was analyzed over 14 days (Figure 3). On Day 1, following encapsulation, U87 cells started with a rounded morphology in all groups. By Day 8, in 50% and 100% MMP-degradable hydrogels, extensive cell spreading was observed, and these cell processes continued to elongate over 14 days. In contrast, in 0% MMP-degradable hydrogels, tumor cells remained rounded after 14 days in culture. Staining for cytoskeletal F-actin on Day 14 confirmed the brightfield microscopy observations (Figure 4, Supplementary Videos S1 – S3). As seen in 0% MMP-degradable gels, tumor cell aggregates remained rounded, whereas in 50% and 100% MMP-degradable hydrogels, extensive actin-rich cell protrusions from tumor mass were observed (animated confocal images of tumor cells in 0%, 50% and 100% MMP-degradable hydrogels are provided in Supplementary Videos S1, S2, and S3, respectively).

Effects of MMP-degradability on ECM remodeling and synthesis

To analyze the effects of MMP-degradability on ECM remodeling, the gene expression levels of MMPs (MMP1, 2, and 9) were measured using quantitative RT-PCR (Figures 5A – C). After 14 days in culture, all hydrogel formulations supported expression of MMP1 and MMP9. The greatest increase in expression was observed for MMP1 (36 – 46 fold, as compared to Day 1), followed by MMP9 (15 – 20 fold, as compared to Day 1). Minimal changes were observed for MMP2. Moreover, changing the percentage of MMP-degradable crosslinks did not further alter MMP expression.

To analyze the effects of MMP-degradability on ECM synthesis, the expression of different isoforms HA synthases (HAS1, HAS2, and HAS3) was measured (Figures 5D – F) using quantitative RT-PCR. Only HAS2 was highly upregulated over 14 days (12 – 15 fold, as compared to Day 1), and minimal changes were observed for HAS1 and HAS3. Changing the percentage of MMP-degradable crosslinks did not change HAS expression.

DISCUSSION

Matrix degradation via MMPs is an important prerequisite for GBM cell invasion, which drives tumor progression *in vivo*.[17] Enhanced expression of MMP1 has been correlated with the degree of tumor malignancy, and MMP2 and MMP9 have been found at GBM cell invadopodia at the tumor periphery, highlighting the importance of MMPs in driving tumor development.[15,26] We recently reported a MMP-degradable, PEG-based hydrogel platform for 3D culture of GBM cells as *in vitro* tumor model.[11] How the degree of MMP-degradability affects GBM cell proliferation and spreading remains unknown. Here we sought to investigate the effects of MMP-degradability on GBM cell behavior to identify an

optimal formulation that can support GBM cell proliferation and spreading. The percentage of MMP-degradable crosslinks (0%, 50%, and 100%) in PEG-based hydrogels was modulated by tuning the ratio of non-degradable PEG crosslinker and MMP-degradable crosslinker. The MMP-degradable crosslinker selected for this study has been shown to be degraded by GBM-relevant MMPs (MMP1, 2, and 9).[18] Using an immortalized GBM cell line (U87) as a model cell type, we demonstrated that all hydrogel formulations with varying percentages of MMP-degradable crosslinks supported robust U87 cell proliferation. However, cell spreading was only observed in 50% and 100% MMP-degradable hydrogels, suggesting that MMP-degradability is required for GBM cell spreading in 3D. 50% and 100% MMP-degradable hydrogels supported cell spreading in a comparable manner, suggesting that 50% MMP-degradable crosslinks may be a suitable formulation for *in vitro* brain tumor models.

A key hallmark of cancer, including GBM, is abnormal, excessive cell proliferation. In this study, all three hydrogel formulations with varying MMP-degradability supported robust proliferation of U87 cells, up to 10 fold after 14 days (Figure 1C). One striking difference between our results and previous hydrogel systems is a significantly higher fold change in cell proliferation over time in our PEG-based hydrogels. For example, in a gelatin-based hydrogel platform for U87 cell culture, cell proliferation over 14 days was less than 2 fold.[9] In a HA and gelatin composite hydrogel system, U87 cells proliferated less than 3 fold after 14 days.[27] Our hydrogel platform may be more permissive for cell proliferation for a number of reasons, including differences in the hydrogel stiffness and mechanisms of MMP-mediated degradation of hydrogel crosslinks. First, in this study, the initial stiffness of hydrogels with varying MMP-degradability ranged from 1.2 to 2.0 kPa, which is within the range reported for normal human brain tissue.[24,25] Previous hydrogel systems had stiffnesses ranging from 2.0 kPa to over 50 kPa, which is significantly stiffer than brain tissue.[9,27] Moreover, in our hydrogel platform, a MMP-degradable peptide was used for hydrogel crosslinking and for cell-mediated matrix degradation. The peptide selected has been shown to be degraded by GBM-relevant MMPs, MMP1, MMP2, and MMP9.[18] Previous hydrogel platforms utilized gelatin for hydrogel fabrication and cell-mediated MMP degradation. The speed and specificity of cell-mediated degradation of our MMP-degradable peptide and the previously used gelatin polymer may be significantly different, resulting in differential cell proliferation responses. Interestingly, MMP-degradability did not seem to be required for U87 cell proliferation in PEG hydrogels, as all hydrogel formulations supported robust proliferation (up to 10 fold, as compared to Day 1). This result suggests that GBM cells can resist local stress and proliferate in a non-degradable microenvironment. Previous literature has shown that GBM cells can change their cell shape in order to adapt and squeeze through confined spaces,[28,29] suggesting that matrix degradability may not be a pre-requisite for cell proliferation in 3D hydrogels. It is important to note that U87 is an immortalized cell line, and the immortalization process is known to alter tumor cell phenotypes relative to the patient samples.[30] Future studies will investigate if primary patient-derived tumor cells display the same response to MMP-degradability. Furthermore, although the MMP peptide selected can be degraded by GBM-secreted MMPs, the effects of the peptide sequence on tumor cell fates remains to be investigated.

Although U87 cells were able to robustly proliferate regardless of MMP degradability, cell spreading was highly sensitive to MMP degradability. In 50% and 100% MMP-degradable hydrogels, significantly more cell protrusions were observed by Day 8, resulting in extensive cell spreading and actin-rich cell processes by Day 14 (Figures 3 and 4, Supplementary Videos S1 – S3). In contrast, in 0% MMP-degradable hydrogels, U87 cells were unable to remodel the surrounding matrix and thus remained largely rounded. The lack of cell spreading in 0% degradable hydrogels was not due to a deficiency in ECM remodeling, as comparable gene expression levels of various MMPs were observed for hydrogels with varying percentages of MMP-degradability (Figure 5A – C). Instead, increased physical restriction and confinement of cells due to the lack of degradable crosslinks may be the dominating factor in preventing cell spreading. There are two main mechanisms by which cells migrate in 3D matrices, including mesenchymal migration, which depends on proteolytic ECM degradation, and amoeboid migration, in which cells change their morphology to move through confined spaces.[6] Using the Flory-Rehner calculation and the equilibrium swelling ratio, we calculated the theoretical mesh sizes of hydrogels with varying MMP degradability to be ranging from 14.72 to 15.18 nm, which is several orders of magnitude smaller than the size of cells. Previous reports have suggested that mesh sizes in this range are prohibitive of amoeboid mode of migration.[31] As such, the mesenchymal mode is likely the way by which GBM cells migrate and invade inside 3D hydrogels. Such behavior has been observed in GBM cells cultured in 3D collagen gels, organotypic brain slices, and in vivo mouse models, in which GBM cells exhibited mesenchymal mode of migration with polarized extensions at the leading membrane edge.[13]

In order to spread and migrate within 3D matrices, GBM cells secrete MMPs to degrade ECM proteins. Our hydrogel platform supported significant upregulation of MMP1 and MMP9 expression levels by Day 14 in all groups (Figure 5A and C). Minimal changes in MMP2 expression were observed over time in all groups (Figure 5B). Varying MMP-degradability did not further alter MMP expression levels. MMP1 is a collagenase known to cleave collagen types I, II, III, VII, and X, gelatin, entactin, aggrecan, and tenascin.[32] Immunostaining of MMP1 within GBM tumors found significant expression in the invasive zone of the tumor, mostly around tumor cells and not within the ECM.[15] MMP9 is a gelatinase, which degrades gelatin and collagen types IV and V. Previous literature has found MMP9 to play roles in GBM cell invasion, in addition to regulating the availability of vascular endothelial growth factor (VEGF), which plays pivotal roles in tumor angiogenesis.[33] After 7 days in culture in composite GelMA/PEGDA hydrogels, previous literature found similar upregulation of MMP9 (20 fold) for U87 cells relative to 2D culture.[9] MMP2 is also a gelatinase that degrades the same substrates as MMP9, but MMP2 more efficiently degrades fibronectin compared to MMP9.[34] In addition to ECM remodeling via degradation, GBM cells can also deposit their own matrix and secrete ECM proteins, such as HA via HA synthases (HAS). HAS2 expression was highly upregulated in all groups, up to 15 fold by Day 14. Minimal changes in HAS1 and HAS3 expression levels were observed in all groups. Varying the percentage of MMP-degradable crosslinks did not significantly change the expression of various HAS isoforms. HAS1 and HAS3 are responsible for synthesizing HA of molecular weight 2×10^5 to 2×10^6 kDa, while HAS2 is responsible for HA of molecular weight greater than 2×10^6 kDa.[35] The molecular weight

of HA has been found to play differential roles in glioma cell proliferation and migration.[17] Previous literature has found also that overproduction of HA by HAS2 can enhance anchorage-independent growth tumor cell proliferation.[36] Although varying the percentage of MMP-degradable crosslinks did not alter MMP and HAS expression levels, gene expression is a one-time snapshot, and possible differences in gene expression may occur at alternative timepoints and for other signaling pathways.

A key hallmark of GBM tumor cells is their extreme ability to migrate and disseminate throughout brain tissue, precluding complete surgical resection and leading to eventual tumor recurrence. To determine an optimal hydrogel formulation that facilitates MMP-mediated GBM invasion, here we investigated the effects of varying the percentage of MMP-degradable crosslinks (0%, 50%, and 100%) in PEG hydrogels on GBM cell proliferation and spreading. All hydrogels supported robust tumor cell proliferation and upregulation of gene expression of ECM-remodeling proteins, namely MMP1, MMP2, and HAS2. MMP-degradability was required for tumor cell spreading, as no spreading was observed in 0% MMP-degradable. In contrast, 50% and 100% MMP-degradable hydrogels supported robust cell spreading in a comparable manner, suggesting 50% degradation is sufficient for engineering 3D *in vitro* GBM models that can support tumor cell proliferation and spreading. Our findings highlight the importance of modulating MMP-degradability to facilitate brain tumor cell fates in 3D niches and may be applied when engineering *in vitro* models for other cancer types.

Acknowledgments

This work was supported by the following grants: NIH R01DE024772 (F.Y.), NSF CAREER award (CBET-1351289) (F.Y.), and California Institute for Regenerative Medicine Tools and Technologies Award (RT3-07804) (F.Y.). The authors also acknowledge funding from the Stanford Child Health Research Institute Faculty Scholar Award (F.Y.), Stanford Bio-X IIP grant award (F. Y.), the Alliance for Cancer Gene Therapy Young Investigator award grant (F.Y.)., and the Stanford Chem-H Institute (F.Y.). C.W. would like to thank Stanford Graduate Fellowship and Stanford Interdisciplinary Graduate Fellowship for support. The authors would like to thank Prof. Gerald Grant and Prof. Michelle Monje for valuable discussions. The authors also appreciate technical assistance from Stanford Cell Sciences Imaging Facility for confocal imaging and Anthony Behn for mechanical testing.

References

1. Krex D, Klink B, Hartmann C, von Deimling A, Pietsch T, Simon M, Sabel M, Steinbach JP, Heese O, Reifenberger G, et al. Long-term survival with glioblastoma multiforme. Brain. 2007; 130(10): 2596–2606. [PubMed: 17785346]
2. McLendon RE, Halperin EC. Is the long-term survival of patients with intracranial glioblastoma multiforme overstated? Cancer. 2003; 98(8):1745–1748. [PubMed: 14534892]
3. Wen PY, Kesari S. Malignant Gliomas in Adults. New England Journal of Medicine. 2008; 359(5): 492–507. [PubMed: 18669428]
4. Berens ME, Giese A. "…those left behind." Biology and Oncology of Invasive Glioma Cells. Neoplasia (New York, NY). 1999; 1(3):208–219.
5. Ananthanarayanan B, Kim Y, Kumar S. Elucidating the mechanobiology of malignant brain tumors using a brain matrix-mimetic hyaluronic acid hydrogel platform. Biomaterials. 2011; 32(31):7913–7923. [PubMed: 21820737]
6. Pathak A, Kumar S. Biophysical regulation of tumor cell invasion: moving beyond matrix stiffness. Integrative Biology. 2011; 3(4):267. [PubMed: 21210057]

7. Ulrich TA, de Juan Pardo EM, Kumar S. The Mechanical Rigidity of the Extracellular Matrix Regulates the Structure, Motility, and Proliferation of Glioma Cells. Cancer Research. 2009; 69(10): 4167–4174. [PubMed: 19435897]
8. Pedron S, Becka E, Harley BA. Regulation of glioma cell phenotype in 3D matrices by hyaluronic acid. Biomaterials. 2013; 34(30):7408–17. [PubMed: 23827186]
9. Pedron S, Harley BAC. Impact of the biophysical features of a 3D gelatin microenvironment on glioblastoma malignancy. Journal of Biomedical Materials Research Part A. 2013 n/a-n/a.
10. Kaufman LJ, Brangwynne CP, Kasza KE, Filippidi E, Gordon VD, Deisboeck TS, Weitz DA. Glioma Expansion in Collagen I Matrices: Analyzing Collagen Concentration-Dependent Growth and Motility Patterns. Biophysical Journal. 2005; 89(1):635–650. [PubMed: 15849239]
11. Wang C, Tong X, Yang F. Bioengineered 3D Brain Tumor Model To Elucidate the Effects of Matrix Stiffness on Glioblastoma Cell Behavior Using PEG-Based Hydrogels. Molecular Pharmaceutics. 2014
12. Viapiano, MS., Lawler, SE. Glioma Invasion: Mechanisms and Therapeutic Challenges. In: Meir, GE., editor. CNS Cancer: Models, Markers, Prognostic Factors, Targets, and Therapeutic Approaches. Totowa, NJ: Humana Press; 2009. p. 1219-1252.
13. Zhong J, Paul A, Kellie SJ, O'Neill GM. Mesenchymal Migration as a Therapeutic Target in Glioblastoma. Journal of Oncology. 2010; 2010:430142. [PubMed: 20652056]
14. Rao JS. Molecular mechanisms of glioma invasiveness: the role of proteases. Nature Reviews Cancer. 2003; 3(7):489–501. [PubMed: 12835669]
15. Stojic J, Hagemann C, Haas S, Herbold C, Kühnel S, Gerngras S, Roggendorf W, Roosen K, Vince GH. Expression of matrix metalloproteinases MMP-1, MMP-11 and MMP-19 is correlated with the WHO-grading of human malignant gliomas. Neuroscience Research. 2008; 60(1):40–49. [PubMed: 17980449]
16. Hagemann C, Anacker J, Haas S, Riesner D, Schömig B, Ernestus R-I, Vince GH. Comparative expression pattern of Matrix-Metalloproteinases in human glioblastoma cell-lines and primary cultures. BMC Research Notes. 2010; 3(1):293. [PubMed: 21067565]
17. Wiranowska, M., Rojiani, MV. Extracellular matrix microenvironment in glioma progression. In: Ghosh, A., editor. Glioma - Exploring Its Biology and Practical Relevance. Intech; 2011. p. 257-284.
18. Patterson J, Hubbell JA. Enhanced proteolytic degradation of molecularly engineered PEG hydrogels in response to MMP-1 and MMP-2. Biomaterials. 2010; 31(30):7836–7845. [PubMed: 20667588]
19. Fairbanks BD, Schwartz MP, Halevi AE, Nuttelman CR, Bowman CN, Anseth KS. A Versatile Synthetic Extracellular Matrix Mimic via Thiol-Norbornene Photopolymerization. Advanced Materials. 2009; 21(48):5005–5010. [PubMed: 25377720]
20. Anderson SB, Lin C-C, Kuntzler DV, Anseth KS. The performance of human mesenchymal stem cells encapsulated in cell-degradable polymer-peptide hydrogels. Biomaterials. 2011; 32(14): 3564–3574. [PubMed: 21334063]
21. Shu XZ, Liu Y, Luo Y, Roberts MC, Prestwich GD. Disulfide Cross-Linked Hyaluronan Hydrogels. Biomacromolecules. 2002; 3(6):1304–1311. [PubMed: 12425669]
22. Delpech B, Maingonnat C, Girard N, Chauzy C, Maunoury R, Olivier A, Tayot J, Creissard P. Hyaluronan and Hyaluronectin in the Extracellular Matrix of Human Brain Tumor Stroma. European Journal of Cancer. 1993; 29(7):1012–1017.
23. Zustiak SP, Leach JB. Hydrolytically Degradable Poly(Ethylene Glycol) Hydrogel Scaffolds with Tunable Degradation and Mechanical Properties. Biomacromolecules. 2010; 11(5):1348–1357. [PubMed: 20355705]
24. Glaser KJ, Manduca A, Ehman RL. Review of MR elastography applications and recent developments. Journal of Magnetic Resonance Imaging. 2012; 36(4):757–774. [PubMed: 22987755]
25. Engler AJ, Sen S, Sweeney HL, Discher DE. Matrix Elasticity Directs Stem Cell Lineage Specification. Cell. 2006; 126(4):677–689. [PubMed: 16923388]
26. Stylli SS, Kaye AH, Lock P. Invadopodia: At the cutting edge of tumour invasion. Journal of Clinical Neuroscience. 2008; 15(7):725–737. [PubMed: 18468901]

27. Heffernan JM, Overstreet DJ, Le LD, Vernon BL, Sirianni RW. Bioengineered Scaffolds for 3D Analysis of Glioblastoma Proliferation and Invasion. Ann Biomed Eng. 2015; 43(8):1965–77. [PubMed: 25515315]

28. Beadle C, Assanah MC, Monzo P, Vallee R, Rosenfeld SS, Canoll P. The role of myosin II in glioma invasion of the brain. Mol Biol Cell. 2008; 19(8):3357–68. [PubMed: 18495866]

29. Cuddapah VA, Robel S, Watkins S, Sontheimer H. A neurocentric perspective on glioma invasion. Nat Rev Neurosci. 2014; 15(7):455–65. [PubMed: 24946761]

30. Li A, Walling J, Kotliarov Y, Center A, Steed ME, Ahn SJ, Rosenblum M, Mikkelsen T, Zenklusen JC, Fine HA. Genomic changes and gene expression profiles reveal that established glioma cell lines are poorly representative of primary human gliomas. Mol Cancer Res. 2008; 6(1):21–30. [PubMed: 18184972]

31. Schwartz MP, Fairbanks BD, Rogers RE, Rangarajan R, Zaman MH, Anseth KS. A synthetic strategy for mimicking the extracellular matrix provides new insight about tumor cell migration. Integrative Biology. 2010; 2(1):32–40. [PubMed: 20473410]

32. McCready J, Broaddus WC, Sykes V, Fillmore HL. Association of a single nucleotide polymorphism in the matrix metalloproteinase-1 promoter with glioblastoma. International Journal of Cancer. 2005; 117(5):781–785. [PubMed: 15957163]

33. Bergers G, Brekken R, McMahon G, Vu TH, Itoh T, Tamaki K, Tanzawa K, Thorpe P, Itohara S, Werb Z, et al. Matrix metalloproteinase-9 triggers the angiogenic switch during carcinogenesis. Nat Cell Biol. 2000; 2(10):737–744. [PubMed: 11025665]

34. Frankowski H, Gu Y-H, Heo JH, Milner R, del Zoppo GJ. Use of Gel Zymography to Examine Matrix Metalloproteinase (Gelatinase) Expression in Brain Tissue or in Primary Glial Cultures. Methods in molecular biology (Clifton, NJ). 2012; 814:221–233.

35. Itano N, Kimata K. Mammalian Hyaluronan Synthases. IUBMB Life. 2002; 54:195–199. [PubMed: 12512858]

36. Kosaki R, Watanabe K, Yamaguchi Y. Overproduction of Hyaluronan by Expression of the Hyaluronan Synthase Has2 Enhances Anchorage-independent Growth and Tumorigenicity. Cancer Research. 1999; 59(5):1141–1145. [PubMed: 10070975]

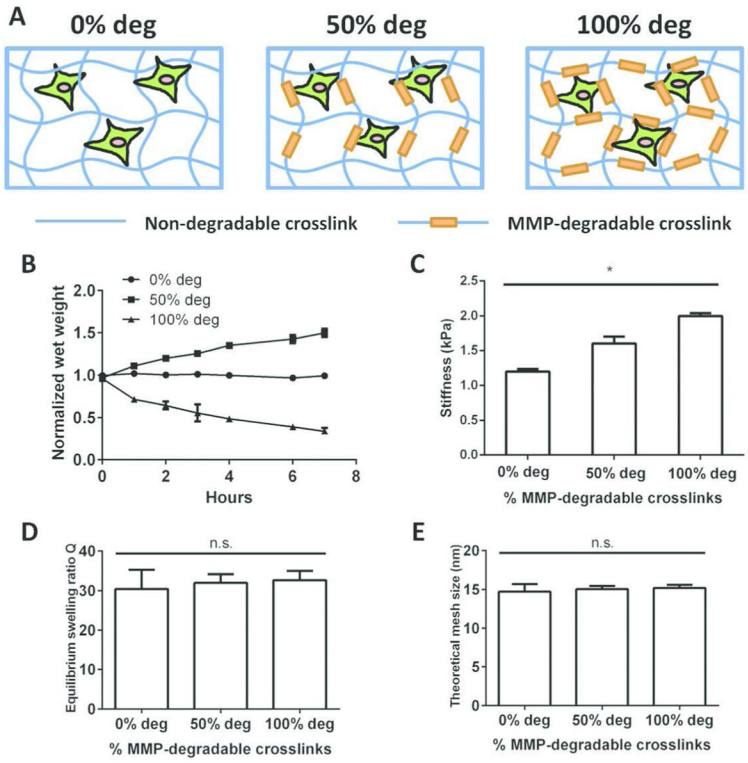

FIG. 1.

(**A**) MMP-degradability of PEG hydrogels was varied by tuning the percentage of MMP-degradable crosslinks (0%, 50%, and 100%). Immortalized adult GBM cell line, U87, was used as model cell type and encapsulated in hydrogels. (**B**) Hydrogel degradation in collagenase solution, as measured by hydrogel wet weight over time normalized to PBS control (n = 3). 0% MMP-degradable gels did not change in weight over time. 50% MMP-degradable gels increased in weight due to hydrogel swelling as crosslinks are degraded. 100% MMP-degradable gels decreased in weight due to mass loss. (**C**) Effects of varying percentage of MMP-degradable crosslinks on hydrogel stiffness, as measured using unconfined compression test (n = 3). * $p < 0.05$. (**D**) Effects of varying percentage of MMP-degradable crosslinks on equilibrium swelling ratio Q, as calculated by the ratio of hydrogel wet weight to hydrogel dry weight. (**E**) Effects of varying percentage of MMP-degradable crosslinks on theoretical mesh size, as calculated from equilibrium swelling ratio Q and Flory-Rehner calculation.

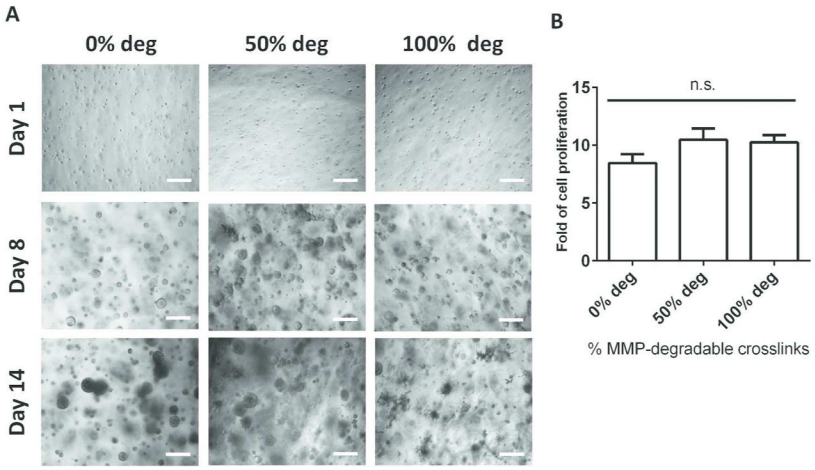

FIG. 2.

All hydrogel formulations supported robust tumor cell proliferation over 14 days. (**A**) Brightfield microscopy of tumor aggregates in 3D hydrogels of varying percentages of MMP-degradable crosslinks. Scale bar = 200 μm. (**B**) Fold of cell proliferation by Day 14 in hydrogels of varying MMP-degradability, calculated from Days 1 and 14 DNA content (n = 3). (n.s. not significant, *$p < 0.05$).

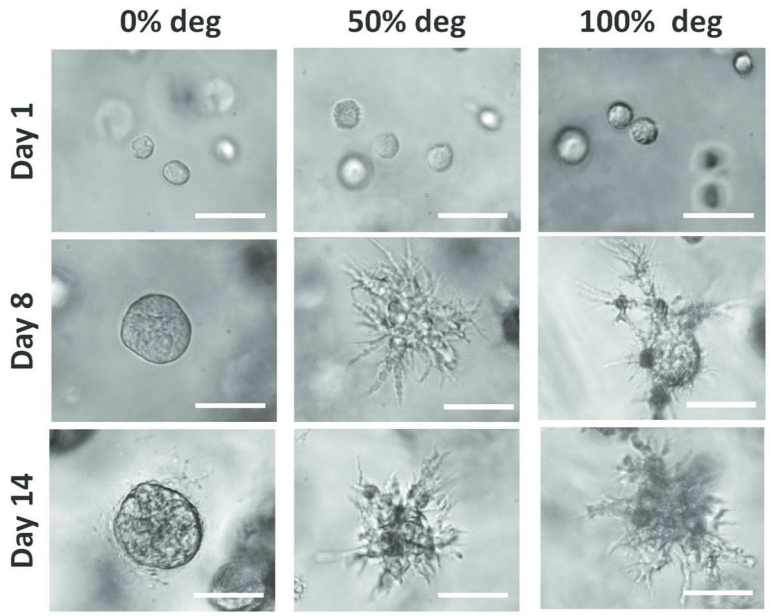

FIG. 3.

Extensive cell spreading was observed in 50% and 100% MMP-degradable hydrogels. Brightfield microscopy of tumor cell morphology in 3D hydrogels of varying percentages of MMP-degradable crosslinks. Scale bar = 50 μm.

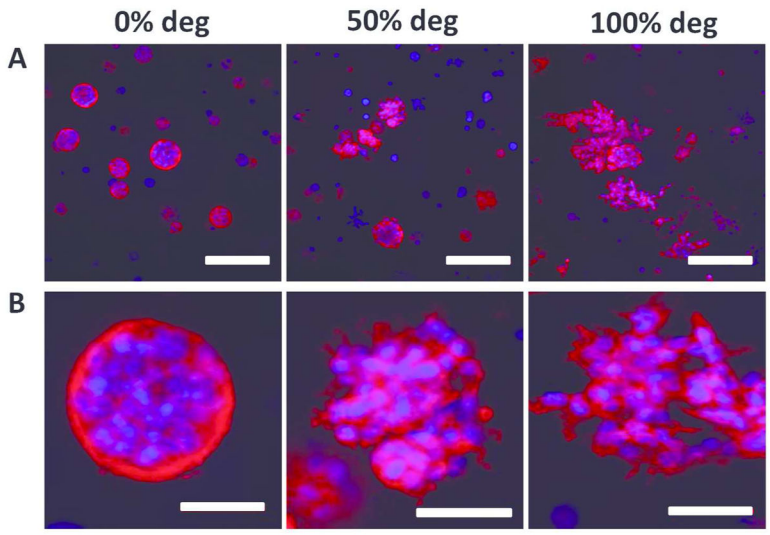

FIG. 4.

Tumor cells displayed extensive F-actin-rich protrusions in 50% and 100% MMP-degradable gels, which were largely absent in 0% MMP-degradable gels. Confocal Z-stack maximal projection of tumor cell F-actin staining in 3D hydrogels of varying percentages of MMP-degradable crosslinks on Day 14. (**A**) Scale bar = 200 μm. (**B**) Scale bar = 50 μm. Blue = nuclei. Red = F-actin.

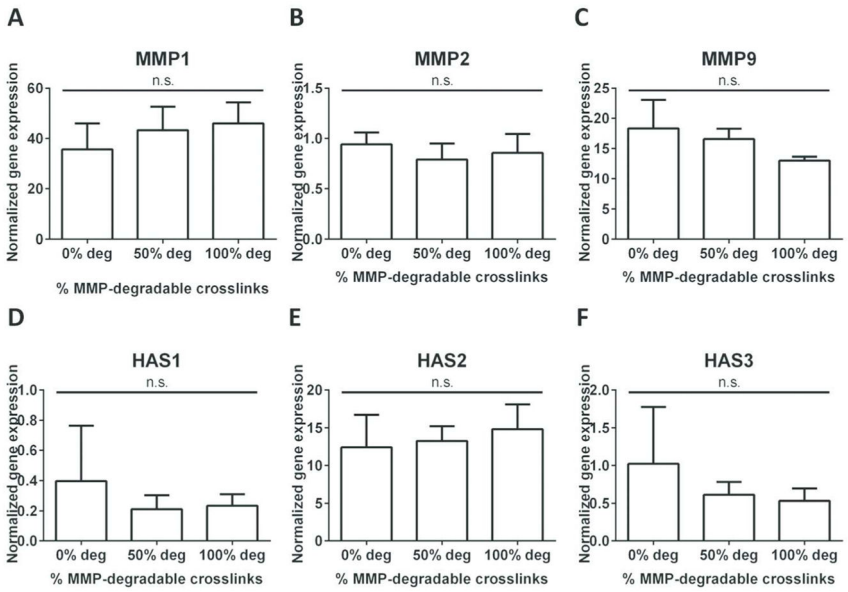

FIG. 5.

All hydrogel formulations supported upregulation of MMP1, MMP9, and HAS2. Changing the percentage of MMP-degradable crosslinks did not further alter gene expression. Fold change in gene expression (n = 3) for MMPs ((**A**) MMP1, (**B**) MMP2, (**C**) MMP9) and HA synthases ((**D**) HAS1, (**E**) HAS2, (**F**) HAS3), on Day 14 normalized to Day 1. (n.s. not significant, *$p < 0.05$).